An efficient *in vivo*-inducible CRISPR interference system for group A *Streptococcus* genetic analysis and pathogenesis studies

Elisabet Bjånes[1,#], Alexandra Stream[1,2,#], Paddy S. Gibson[3], Afonso M. Bravo[3], Samira Dahesh[1], Jonathon L. Baker[4,5], Andrew Varble[6], Victor Nizet[1,2,*], Jan-Willem Veening[1,3,*]

[1]Department of Pediatrics, University of California San Diego, La Jolla, CA, USA

[2]Skaggs School of Pharmacy and Pharmaceutical Sciences, University of California San Diego, La Jolla, CA, USA

[3]Department of Fundamental Microbiology, Faculty of Biology and Medicine, University of Lausanne, Lausanne, Switzerland

[4]Department of Oral Rehabilitation & Biosciences, School of Dentistry, Oregon Health & Science University, Portland, OR, USA

[5]Genomic Medicine Group, J. Craig Venter Institute, La Jolla, CA, USA

[6]University of Rochester Medical Center, School of Medicine and Dentistry, Rochester, New York, USA

[#]Contributed equally

*Correspondence to Jan-Willem Veening: Jan-Willem.Veening@unil.ch, tel: +41 (0)21 6925625, or Victor Nizet: vnizet@health.ucsd.edu, tel +1 (858) 534-7408

Abstract

While genome-wide transposon mutagenesis screens have identified numerous essential genes in the significant human pathogen *Streptococcus pyogenes* (group A *Streptococcus* or GAS), many of their functions remain elusive. This knowledge gap is attributed in part to the limited molecular toolbox for controlling GAS gene expression and the bacterium's poor genetic transformability. CRISPR interference (CRISPRi), using catalytically inactive GAS Cas9 (dCas9), is a powerful approach to specifically repress gene expression in both bacteria and eukaryotes, but ironically has never been harnessed for controlled gene expression in GAS. In this study, we present a highly transformable and fully virulent serotype M1T1 GAS strain and introduce a doxycycline-inducible CRISPRi system for efficient repression of bacterial gene expression. We demonstrate highly efficient, oligo-based sgRNA cloning directly to GAS, enabling the construction of a gene knockdown strain in just two days, in contrast to the several weeks typically required. The system is shown to be titratable and functional both *in vitro* and *in vivo* using a murine model of GAS infection. Furthermore, we provide direct *in vivo* evidence that the expression of the conserved cell division gene *ftsZ* is essential for GAS virulence, highlighting its promise as a target for emerging FtsZ-inhibitors. Finally, we introduce SpyBrowse (https://veeninglab.com/SpyBrowse), a comprehensive and user-friendly online resource for visually inspecting and exploring GAS genetic features. The tools and methodologies described in this work are poised to facilitate fundamental research in GAS, contribute to vaccine development, and aid in the discovery of antibiotic targets.

Significance statement

While GAS remains a predominant cause of bacterial infections worldwide, there are limited genetic tools available to study its basic cell biology. Here, we bridge this gap by creating a highly transformable, fully virulent M1T1 GAS strain. In addition, we established a tight and titratable doxycycline-inducible system and developed CRISPR interference for controlled gene expression in GAS. We show that CRISPRi is functional *in vivo* in a mouse infection model. Additionally, we present SpyBrowse, an intuitive and accessible genome browser (https://veeninglab.com/SpyBrowse). Overall, this work overcomes significant technical challenges of working with GAS, and together with SpyBrowse, represents a valuable resource for researchers in the GAS field.

Introduction

Streptococcus pyogenes, also known as group A *Streptococcus* (GAS), is a bacterium commonly present in the throat and on the skin (1, 2). This pathogen is notorious for causing strep throat and impetigo, accounting for approximately 700 million non-invasive infections each year (3–5). However, GAS can also lead to serious invasive diseases, including necrotizing fasciitis and streptococcal toxic shock syndrome, resulting in over 150,000 deaths annually (4). Additionally, GAS is the immunological trigger for acute rheumatic fever (ARF) and rheumatic heart disease (RHD), causing substantial death and disability in many developing countries. Despite rising GAS resistance to certain antibiotic classes, the pathogen has fortunately remained susceptible to penicillin and other β-lactam agents (6).

There is presently no commercially available vaccine to protect against GAS infection (7). GAS presents a challenge for vaccine antigen selection due to the variability in the abundant surface-exposed M protein with over 230 *emm* types circulating globally (8). The most common *emm* type, M1, is a major contributor to GAS global epidemiology, and is particularly prominent in severe, invasive infections (9). The search for new GAS antibiotic targets and vaccine candidates is hindered by a knowledge gap in fundamental GAS biology, partly because M1-type GAS strains are exceptionally challenging to manipulate genetically (10, 11). In this study, we present a toolbox for GAS genetic engineering, utilizing the hard-to-transform and clinically relevant M1T1-type strain 5448 (NV1) as

71 model (1, 12). This toolbox should be generally applicable to GAS and related bacteria, encompassing
72 protocols for recombineering using GoldenGate-assembled linear DNA, oligo-based sgRNA cloning, a
73 titratable doxycycline-inducible promoter, and CRISPR interference (CRISPRi) effective both *in vitro*
74 and *in vivo* in a murine GAS infection model.

75 Additionally, we present SpyBrowse, an intuitive and accessible genome browser
76 (https://veeninglab.com/SpyBrowse), based on JBrowse (13), a graphical and user-friendly interface to
77 explore the GAS genomic landscape with direct linking to UniProt (14) and other useful resources such
78 as PaperBlast (15). Overall, this work overcomes significant technical challenges of working with GAS,
79 facilitating genetic engineering and targeted gene knockdowns to advance our insights into the
80 physiology and cell biology of this preeminent human bacterial pathogen.

81

82 **Results**

83 **Improved transformability of GAS M1T1 Strain 5448 by mutating *hsdR***

84 GAS5448, a widely used strain in fundamental research, serves as a clinical representative of the
85 globally distributed M1T1 serotype associated with severe invasive infections. While 5448 has been
86 effectively employed in murine models of GAS infection (16, 17), its genetic manipulation poses
87 challenges, with even the construction of transposon mutant libraries proving highly difficult (10, 11,
88 18). To enhance GAS 5448 transformation efficiencies while retaining full virulence, we targeted one
89 of the major barriers to transformation—the HsdR restriction subunit of the conserved three-component
90 Type I restriction-modification (RM) system, HsdRSM. *Hsd,* denoting Host specificity of DNA,
91 signifies how these Type I RM systems cleave intracellular (foreign) DNA with improper methylation
92 patterns. Mutations in this system improve transformation efficiency in other GAS strains (19–22), but
93 with potential pleiotropic consequences. For example, while deletion of the entire *hsdRSM* system in
94 serotype M28 GAS strain MEW123 boosted transformation efficiency, it concurrently reduced
95 virulence in a murine model of infection (20). Similarly, attenuated virulence was seen in a
96 spectinomycin marker-replacement mutant eliminating just the restriction subunit *hsdR*, likely due to
97 polar effects leading to partially methylated genomic DNA (20).

98 To address the above obstacles, we generated a mutant of *hsdR* in the wild-type (WT) GAS
99 5448 (strain NV1, Table S2) using an erythromycin resistance cassette. This cassette, previously
100 demonstrated to provide selectable resistance at very low transcription levels without requiring an
101 upstream promoter (23), was introduced using GoldenGate assembly combined with recombineering
102 (Fig. 1A-B, strain NV28: *hsdR::ery*, see Methods for details). SMRT sequencing (PacBio) confirmed
103 the desired mutation in NV28, and the identical genomic DNA methylation pattern to NV1 validating
104 the absence of polar effects from the erythromycin cassette replacement. Global DNA methylation
105 patterns analysis suggested that the MTase activity of the HsdRSM system of GAS strain 5448
106 methylates adenines at position 3 in the motifs 5'-GCANNNNNNTTAA'3' and 5'-
107 TTAANNNNNNTGC'3', with all 344 motifs in the NV1 genome methylated, consistent with patterns
108 observed in other M1 strains (21) (Fig. 1C).

109 Moreover, the virulence of the strain harboring the *hsdR::ery* cassette was indistinguishable
110 from its WT parent strain (see below, Fig. 5C). Electroporation transformation efficiency with
111 replicative plasmid pDC123 (24), lacking a putative HsdR restriction site, remained as efficient in the
112 *hsdR::ery* mutant as in the WT. However, when strain NV28 was transformed with replicative plasmid
113 pDC-sgRNA (see below, Fig. 2E), containing a single HsdR site, transformation efficiencies were more
114 than 60-fold higher than transforming pDC-sgRNA to WT NV1 (Fig. 1D). Consequently, the newly
115 constructed GAS M1T1 5448-derived *hsdR::ery* mutant not only allows for increased transformation
116 efficiencies with foreign DNA containing HsdR motifs, but may also serve as a valuable genetic
117 background for future studies.

118 The long-read genome-sequenced NV1 strain was compared to the published 5448 reference
119 genome which was generated by illumina short read sequencing (25), revealing a large inversion of
120 1,475,033 base pairs. This structural variant is flanked by two ISAs1-like element IS1548 family
121 transposase genes, which typically harbor terminal inverted repeats (26). The two transposase genes are
122 oriented in opposing directions and exhibit two single nucleotide polymorphisms. It is highly probable
123 that the short read approach used in the original 5448 genome project contributed to an inaccurate
124 genome assembly. In addition, NV1 contains 6323 additional bases compared to 5448 and several SNPs

125 mainly attributed to the transposase genes (see Methods). Therefore, we propose using the genome

126 assembly presented here for GAS studies involving strain 5448 NV1 (Genbank accession CP140117.2).

127

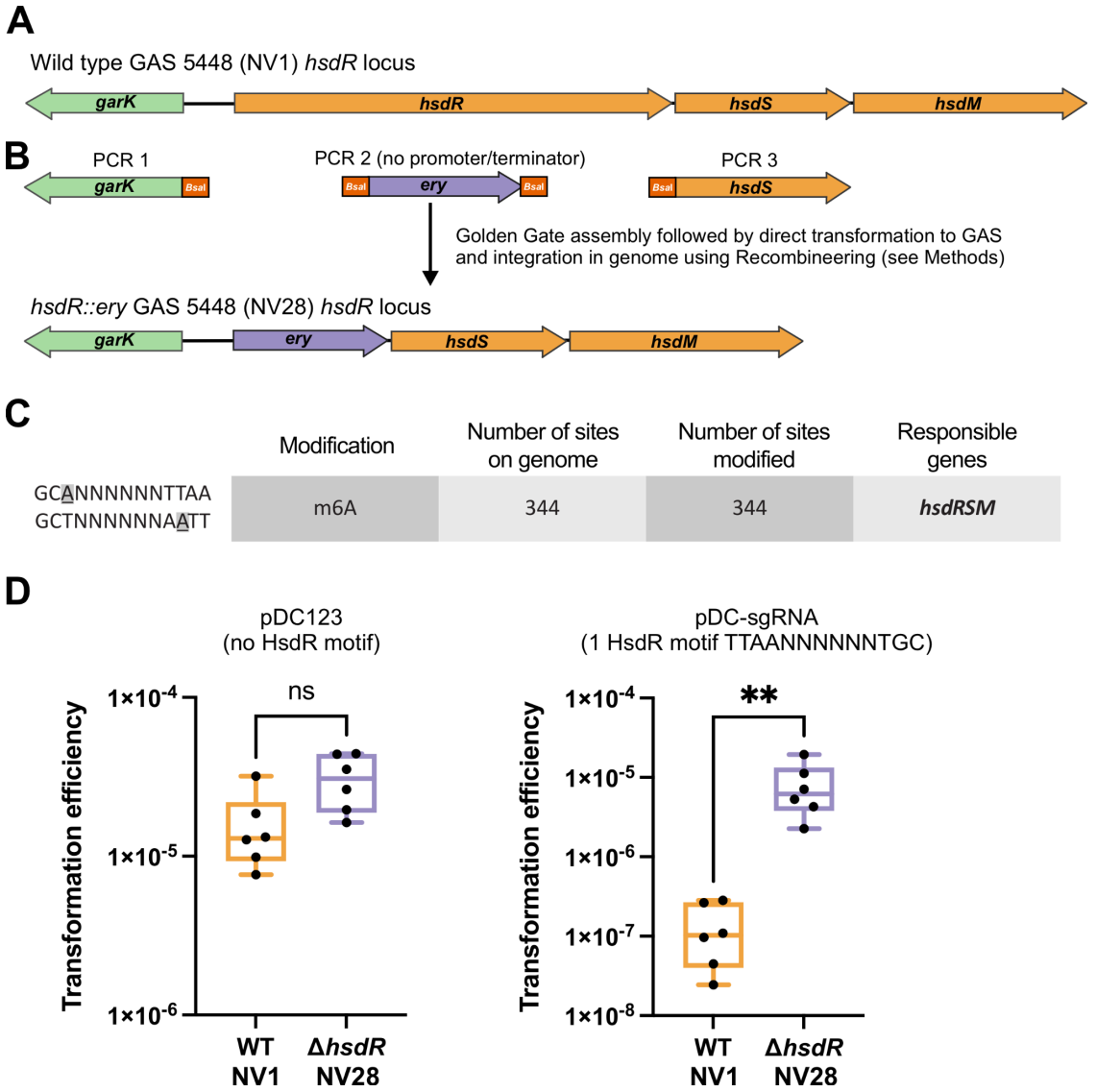

128

129 **Fig. 1: Golden Gate assembly and recombineering to create a highly transformable *hsdR* mutant in M1T1**

130 **GAS strain 5448.** (**A**) Schematic representation of the genomic organization of the *hsdRSM* locus in WT GAS

131 strain M1 5448 (NV1). Gene annotations were made by Prokka (27). (**B**) Three PCRs were performed each

132 containing unique *Bsa*I restriction sites that allow for scarless Golden Gate assembly of a linear fragment in which

133 *hsdR* is replaced by an erythromycin resistance cassette (*ery*). PCR 1 contains 1392 bp upstream of *hsdR*

134 (including the *garK* gene and excluding the start codon of *hsdR*), PCR 2 contains the 785 bp promoterless and

135 terminatorless *ery* cassette (23) flanked by *Bsa*I sites while PCR 3 contains a 1238 bp downstream region of *hsdR*

136 (including its stop codon and *hsdS*). After Golden Gate assembly with *Bsa*I and T4 ligase (see Methods), the

137 resulting 3383 bp ligation product was purified and directly used to transform electrocompetent NV2 (NV1 +
138 pAV488) cells that were grown with 1 mM of IPTG to induce the recombineering system present on plasmid
139 pAV488 resulting in strain NV3 (NV2, *hsdR::ery*). Recombineering of GAS using pAV488 is described in more
140 detail elsewhere (Varble, unpublished). Strain NV3 was plasmid cured resulting in strain NV28 (NV1, *hsdR::ery*).
141 The genomic organization of the *hsdRSM* locus in strain NV28 (*hsdR::ery*) is shown. (**C**) Methylation motifs
142 identified in strains NV1, NV28, and NV6 using SMRT sequencing (see Methods for details). (**D**) Transformation
143 efficiencies of WT GAS 5448 (NV1) and the *hsdR::ery* mutant (NV28) are shown. Left: Strains were transformed
144 with 140 ng (~50 fmol) of plasmid pDC123 (24) that does not contain an HsdR-motif. Right: Strains were
145 transformed with 247 ng (~95 fmol) of plasmid pDC-sgRNA (see **Fig. 2C**) that contains a single HsdR-motif.
146 Each dot represents a replicate and a Kolmogorov-Smirnov test was used to calculate statistical significant
147 differences between the two strains (P value **<0.005).
148

149 **Replacing wild type GAS *cas9* with a doxycycline-inducible dead *cas9* (*dcas9*)**

150 CRISPRi has emerged as a powerful approach for evaluating the functionality of both essential and
151 non-essential genes across a wide range of bacteria (28–31). This gene-silencing technique employs a
152 catalytically inactive version of the GAS Cas9 protein (dCas9) and a single guide RNA (sgRNA). The
153 dCas9-sgRNA complex binds via complementary base pairing of the spacer sequence in the sgRNA to
154 a specific genomic DNA sequence located beside a protospacer adjacent motif (PAM). This binding
155 effectively halts transcription of the target gene and genes within the same operon (**Fig. 2A**) (32, 33).
156 Curiously, while GAS Cas9 is frequently utilized in CRISPRi across various bacteria, as far as we are
157 aware, CRISPRi has not been applied to GAS (34). Our objective in this study is to close this gap and
158 introduce CRISPRi as a valuable tool for investigating gene function in GAS.

159 An optimal CRISPRi system should tightly regulate the expression of a dCas9. However, the
160 selection of suitable inducible promoters for GAS has been limited. The most commonly used system
161 involves a tetracycline-inducible promoter adapted from the Gram-negative bacterium *Escherichia coli*
162 (35, 36). Unfortunately, this system has been reported to exhibit either leakiness or a narrow induction
163 range in GAS (36). In a previous study, we developed a tetracycline, anhydrotetracycline, and
164 doxycycline-inducible CRISPRi system with a highly dynamic range in *S. pneumoniae.* This was
165 achieved by codon optimizing *E. coli tetR,* combined with the selection and counterselection of random

166 promoter libraries containing *tetO* operators (23, 37). Given the similar codon usage between GAS and
167 *S. pneumoniae*, we hypothesized that this TetR-based system could also function effectively in GAS.
168 An additional advantage of this TetR-based system is the excellent tissue penetration of doxycycline
169 (doxy) (38). Our prior work demonstrated the successful delivery of doxy through mouse chow or direct
170 intraperitoneal injection to induce pneumococcal constructs in various mouse body/tissue niches,
171 including the blood and lungs (23, 37, 39).

172 To mitigate potential crosstalk with the intrinsic Cas9-CRISPR system, we strategically chose
173 the WT GAS *cas9* locus as the genomic integration site for stable introduction of the inducible *dcas9*
174 cassette. Using Golden Gate assembly in conjunction with recombineering (see Methods), we first
175 replaced the native *cas9* locus, inclusive of the tracrRNA and the CRISPR spacer array locus, with a
176 kanamycin resistance marker (*kan*), resulting in strain NV4 (**Fig. 2B**). Next, we replaced the *kan* marker
177 of strain NV4 with the *tetM-tetR*-P*tet-dcas9* cassette from *S. pneumoniae* strain VL3469 (37). This
178 cassette imparts tetracycline/doxycycline resistance via the *tetM* marker and positions *dcas9* under the
179 TetR-controlled *S. pneumoniae* P*tet* promoter (23). Finally, the strain underwent curing of the pAV488
180 recombineering plasmid, yielding strain NV6 (**Fig. 2B**). Whole-genome sequencing of strain NV6
181 verified the accurate introduction of all elements (SRA genome accession number SRX22828772).

182

183 **Construction of Gram-positive replicative vector pDC-sgRNA enables efficient sgRNA cloning**

184 Next, we designed a replicative vector tailored for direct sgRNA cloning in GAS. We replaced the *phoZ*
185 reporter gene within the Gram-positive high-copy number (~24 - 90 copies per cell) rolling-circle
186 replication pDC123 plasmid (24, 40) with an *mCherry* cassette flanked by the sgRNA scaffold sequence
187 and Esp3I restriction sites. This configuration allows for Golden Gate assembly or direct ligation of
188 sgRNA spacers using annealed oligonucleotides (**Fig. 2C**). This vector is also capable of replicating in
189 *recA+ E. coli* strains such as MC1061, albeit at low copy numbers (~4 copies per cell)(40). In addition,
190 we incorporated Illumina read 1 and read 2 sequences flanking the sgRNA scaffold to facilitate
191 CRISPRi-seq (41). Notably, we included the +1 of the P3 promoter, ensuring that all cloned spacers
192 initiate with an adenine nucleotide (41). This design promotes efficient transcription and prevents
193 undesirable uridines at the 5' end of the sgRNA (42). Finally, the vector contains a chloramphenicol

194 resistance cassette (*cat*) for selection in GAS (**Fig. 2C**). To validate the functionality of the synthetic
195 P3 promoter (43) in GAS, we transformed pDC-sgRNA into strain NV1, creating NV9. Bacterial
196 examination by fluorescence microscopy revealed strong and uniform mCherry expression in all cells
197 (**Fig. 2D**), confirming the functionality of the P3 promoter in GAS. Given that pDC-sgRNA features
198 the Gram-positive pLS1/pJS3 origin, it is anticipated to be functional across a broad range of Gram-
199 positive bacteria, including but not limited to *Lactococcus lactis*, *Bacillus subtilis*, *S. pneumoniae*,
200 *Enterococcus faecalis* and group B *Streptococcus*.
201

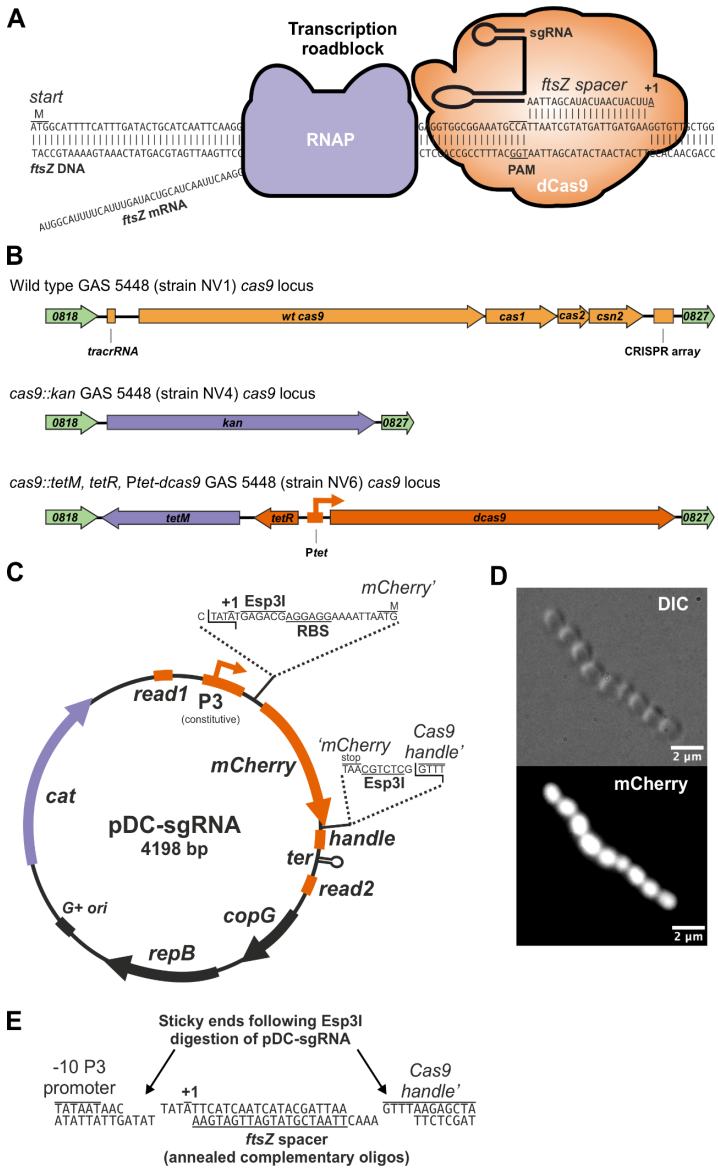

202

203 **Fig. 2: Development of a doxycycline-inducible CRISPRi system for use in Group A Streptococcus.** (**A**)
204 Schematic representation of CRISPRi. An sgRNA encoding a 20 nt spacer region targets dCas9 to the non-

205 template strand containing a protospacer adjacent motif (PAM) on the GAS *ftsZ* locus. Transcription elongation
206 by RNA polymerase (RNAP) is consequently hampered leading to reduced levels of FtsZ in the cell when dCas9
207 is induced. (**B**) Schematic representation of the genomic organization of the *cas9* locus in wildtype GAS strain
208 5448 (NV1), in strain NV4 (*cas9::kan*) and strain NV6 (*cas9::tetM*, *tetR*, Ptet-*dcas9*). (**C**) Schematic
209 representation of sgRNA cloning vector pDC-sgRNA. (**D**) Strain NV9 (NV1, pDC-sgRNA) was grown in THB
210 containing 2 µg/ml of chloramphenicol at 37°C and exponentially growing cells were imaged by differential
211 interference contrast (DIC) and fluorescence microscopy. Scale bar: 2 µm. (**E**) Oligo-based sgRNA cloning in
212 pDC-sgRNA. Plasmid pDC-sgRNA is cut with Esp3I (or its isoschizomer BsmBI) and its resulting sticky ends
213 are shown. Two complementary oligos of each 24 nt long that include a 20 bp spacer sequence are annealed,
214 phosphorylated, ligated and electroporated to competent GAS (see Methods). As an example, the two oligos used
215 to clone the sgRNA targeting GAS *ftsZ* is shown (for oligo design, see Supplementary Table S1). Successful
216 clones lost the *mCherry* cassette and will be white on plate instead of pink.
217

218 **An established pipeline generates unique genome-wide sgRNA spacers for GAS 5448**

219 With the establishment of an inducible *dcas9* strain and an sgRNA expression system for GAS, we
220 systematically designed sgRNA spacer sequences targeting every annotated genetic feature of the GAS
221 5448 genome using our previously established pipeline (41). The algorithm employed for spacer design
222 only designs spacers that exclusively target the non-template strand (**Fig. 2A**) and considers factors
223 such as specificity (to limit off target effects), distance to the start site, and avoiding Esp3I/BsmBI
224 restriction sites (41). Upon running the pipeline, a total of 1823 unique spacers were generated, designed
225 to target 1879 out of 1894 features on the NV1 (5448) genome as annotated by Prokka (27). Suitable
226 spacers could not be identified for 15 genetic elements. Note that certain designed sgRNAs may target
227 more than one genetic element if that element is present in multiple copies (e.g., repeats, gene
228 duplications, etc.). A comprehensive list of all designed sgRNAs is provided in Table S1.
229

SpyBrowse: *Streptococcus pyogenes* (GAS) genome browser

On the basis of the fully closed GAS NV1 genome (Genbank accession CP140117.2), in conjunction with automated genome annotation (see Methods), we have developed a new user-friendly genome browser named SpyBrowse, accessible at https://veeninglab.com/SpyBrowse. SpyBrowse empowers users to conveniently and flexibly search for their gene of interest using either its gene name or locus tag (**Fig. 3A**). Right-clicking on features reveals further information (**Fig. 3B**), including links to Uniprot (including subcellular location predictions and Alphafold protein structure predictions; **Fig. 3C**), PaperBlast (**Fig. 3D**), and NCBI accessions. In addition, SpyBrowse incorporates a track displaying all designed sgRNAs from Table S1.

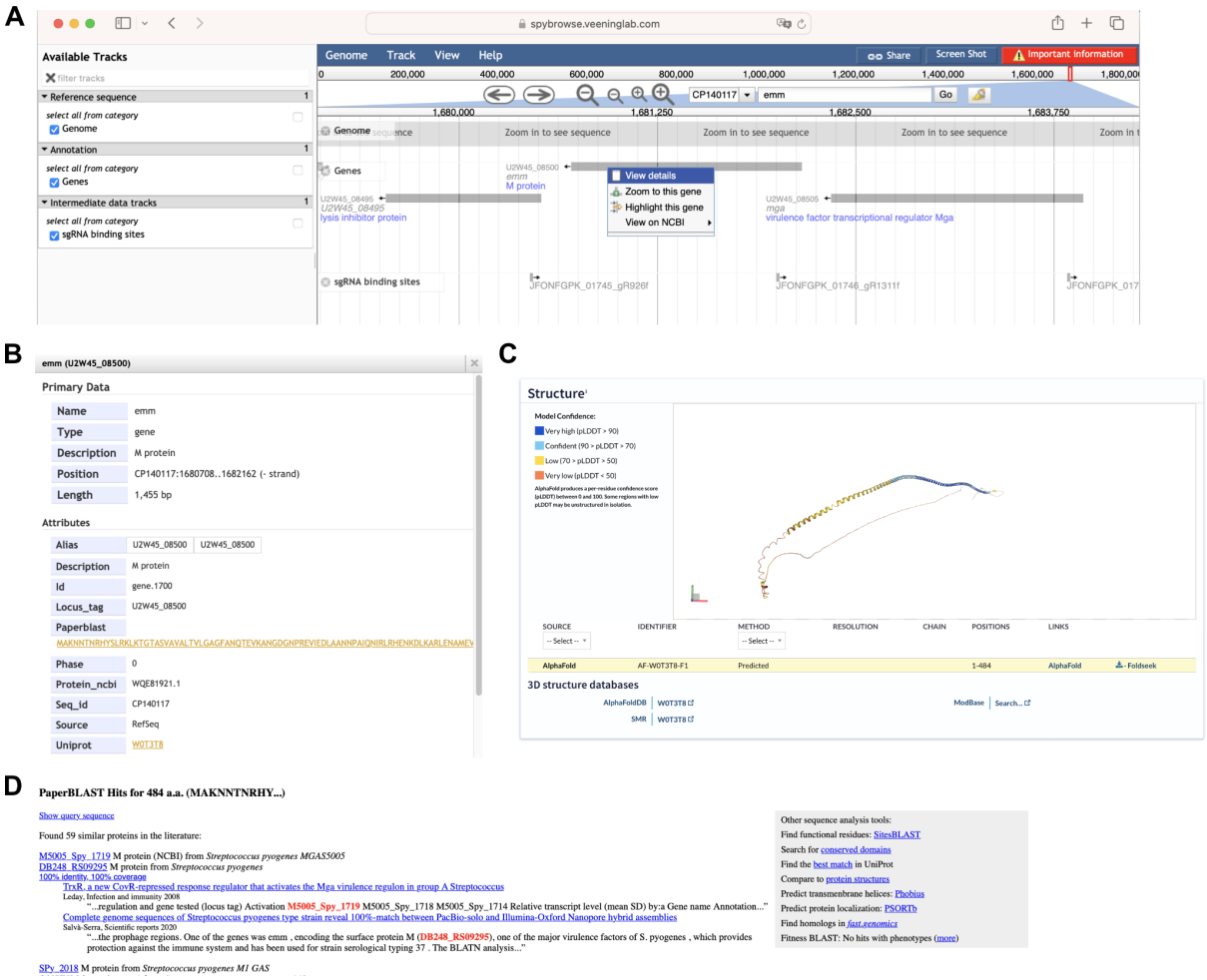

Fig. 3: Spybrowse available at https://veeninglab.com/SpyBrowse. A screenshot of the *emm* locus as shown in SpyBrowse. In the left pane, tracks can be selected. In the right pane, the genome can be browsed via draggin the mouse to the left or right and zooming in and out. Annotated features such as genes and RNAs are shown. The

244 designed spacer targeting the non-template strand of *emm* (JFPNFGPK_01745_gR926f) is shown via the sgRNA
245 binding site track. (**B**) A context menu (upon right-click) provides links to external resources, such as Uniprot
246 (with Alphafold prediction), NCBI (with Blast function) and PaperBlast. (**C**) The predicted Alphafold structure
247 of the M1 protein through the Uniprot link in SpyBrowse is shown. (**D**) The Paperblast hits for the M1 protein are
248 shown.
249

250 **CRISPRi can be used to tunably repress GAS gene expression**

251 To assess the effectiveness of CRISPRi in downregulating the expression of essential genes in GAS,
252 we targeted *dnaA*, which encodes the conserved replication initiator in bacteria, and *ftsZ*, responsible
253 for the conserved tubulin-like cell division protein essential for cell division. FtsZ is a component of
254 the highly conserved division and cell wall (*dcw*) genomic cluster (44). Due to anticipated polar effects
255 of CRISPRi, it is expected that targeting *ftsZ* will also impact transcription of other members of the *dcw*
256 cluster. To construct each sgRNA plasmid, the design outlined in Table S1 was used, and
257 complementary oligos were synthesized for each target. These oligos were annealed, phosphorylated,
258 and ligated in Esp3I-digested pDG-sgRNA (**Figs. 2C, 2E**). Additionally, a control sgRNA was
259 included, containing a random 20-bp sequence (5'-CATACAAGTCGATAGAAGAT-3') that does not
260 match any region in the GAS NV1 5448 genome. The ligation mixtures were directly used to transform
261 electrocompetent GAS NV6 cells (see Methods). Correct clones were cultured in Todd Hewitt broth
262 (THB) within microtiter plates, and the optical density was measured every 10 min. As depicted in **Fig.**
263 **4A**, induction of dCas9 by increasing concentrations of doxycycline (doxy) resulted in reduced growth
264 with the *dnaA* and *ftsZ* sgRNAs. but not with the control sgRNA. Note that at concentrations of 50
265 ng/ml of doxy, a reduction in growth is also observed for the control strain.

266 To confirm the specific targeting of *dnaA* and *ftsZ* by the designed sgRNAs, cells were grown
267 in the presence or absence of 20 ng/ml of doxy for 3h and imaged by microscopy. As anticipated,
268 repression of *dnaA* expression by CRISPRi resulted in cell chaining, with numerous anucleate cells
269 indicative of a failure to initiate DNA replication (**Fig. 4B**). Targeting *ftsZ* led to a distinct block in cell
270 division, resulting in enlarged cells (**Fig. 4B**). These findings collectively show that the CRISPRi
271 system developed for GAS in this study is titratable, specific, and suitable for studying essential genes.

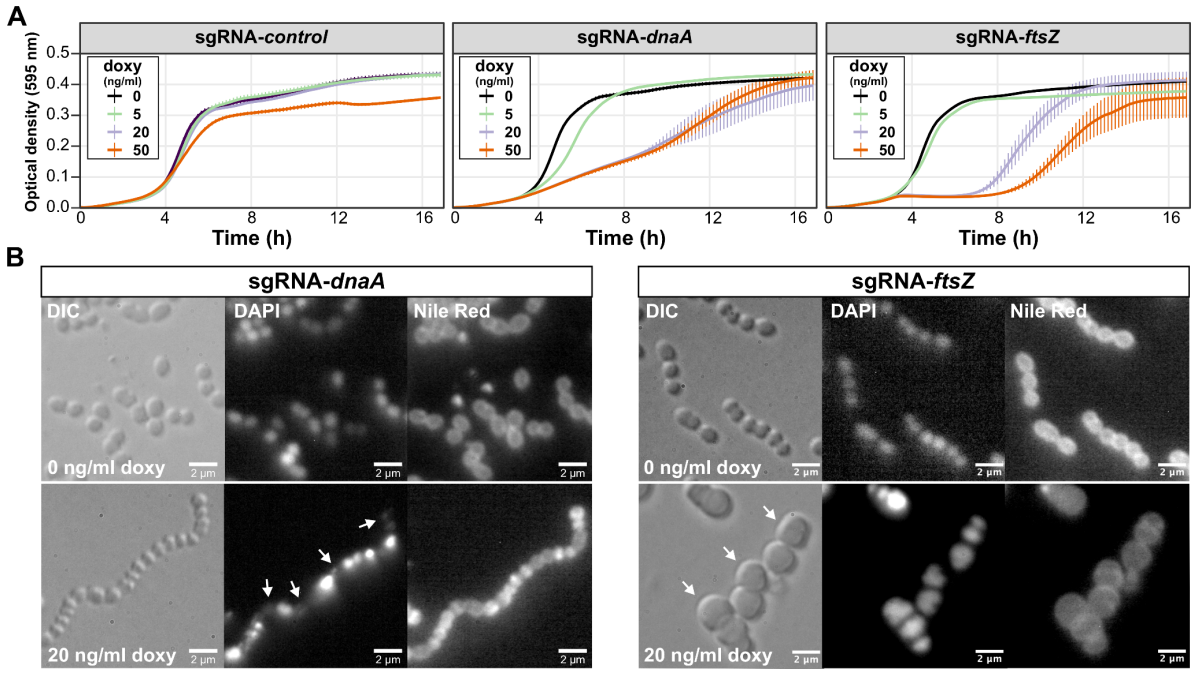

Fig. 4: Targeted repression of *dnaA* and *ftsZ* gene expression by CRISPRi in GAS (**A**) Strains NV26 (NV6+pDC-sgRNA-*control*), NV22 (NV6+pDC-sgRNA-*dnaA*) and NV19 (NV6+pDC-sgRNA-*ftsZ*) were grown in THB containing 2 µg/ml of chloramphenicol at 37°C. Exponentially growing cells were diluted to a start OD of 0.004 in a microtiter plate containing fresh THB with varying concentrations of doxycycline (doxy). The optical density at 595 nm was measured every 10 min. Each line is an average of three replicates with the standard deviation shown. For clarity, the optical density is plotted on a linear scale. (**B**) Strains NV22 and NV19 were grown in the presence or absence of 20 ng/ml of doxy and after 3h, cells were imaged by fluorescence microscopy. DAPI was used to stain the nucleoids and Nile red to stain the membrane. Scale bar: 2 µm. Arrows point to anucleate cells (sgRNA-*dnaA*) or cells with a block in division (sgRNA-*ftsZ*).

CRISPRi to deplete expression of the M protein, a signature GAS virulence factor

To explore the applicability of the CRISPRi system described here for GAS in pathogenesis studies, we initially designed an sgRNA targeting the *emm* gene, encoding the M-protein. As shown in Fig. 5A, the growth of strain NV25 (NV6+pDC-sgRNA-*emm*) was not perturbed by the induction of dCas9 with doxy *in vitro*. Flow cytometry analysis, using an antibody specific to the M1T1 protein, revealed that NV25 induced with doxy exhibited approximately eight-fold less surface-exposed M-protein. This

290 result underscores the precision and efficacy of the CRISPRi-based gene repression system developed
291 for GAS (**Fig. 5B**).
292
293 **CRISPRi targeting of *ftsZ* reveals contribution to *in vivo* GAS virulence**
294 To assess whether the engineered GAS CRISPRi strain NV6 exhibits a comparable virulence profile to
295 the WT 5448 NV1, we intraperitoneally (I.P.) infected outbred CD-1 mice with 1-3 x 10^8 colony-
296 forming units (CFU) and monitored disease progression. As shown in Fig. 5C, no significant difference
297 in mouse survival was observed, demonstrating that the replacement of the CRISPR locus with our
298 CRISPRi cassette, as well as the *hsdR* mutation, had no discernable global impact on systemic virulence.
299 A notable strength of CRISPRi lies in its ability to assess the functionality of essential genes.
300 FtsZ, a highly conserved, tubulin-like, essential cell division protein, represents an attractive target for
301 an expanding list of antibiotic candidates (39, 45). Certain compounds, such as PC190723, are
302 particularly intriguing as they exhibit potent FtsZ inhibitory activity without targeting eukaryotic
303 tubulin (46). While *in vivo* studies have demonstrated the efficacy of several FtsZ inhibitors in clearing
304 bacterial infections, and it is evident that *ftsZ* is essential *in vitro* (**Fig. 4**), direct confirmation of the
305 essentiality of FtsZ or the *dcw* cluster has not been established, to the best of our knowledge. To address
306 this, doxy-treated or mock control mice were challenged I.P. with 1-3 x 10^8 CFU of GAS strain NV19
307 (NV6 + pDC-sgRNA-*ftsZ*) and monitored for disease progression. Doxycycline (25 µg for ~25 mg/kg)
308 or vehicle control were administered I.P. 1h before infection and 48h post-infection. As shown in Fig.
309 5D, 80% of mice that received doxy survived after 14 days compared to only 30% of mock-treated mice
310 ($p = 0.0027$, Mantel-Cox Log Rank test). To ensure that bacterial clearance was not solely attributed to
311 the doxy treatment, an additional control group of mice were infected with strain NV26 (NV6 + pDC-
312 sgRNA-*control*), carrying a non-targeting control sgRNA. No statistically significant difference in
313 survival was observed for this group (**Fig. 5D**).
314

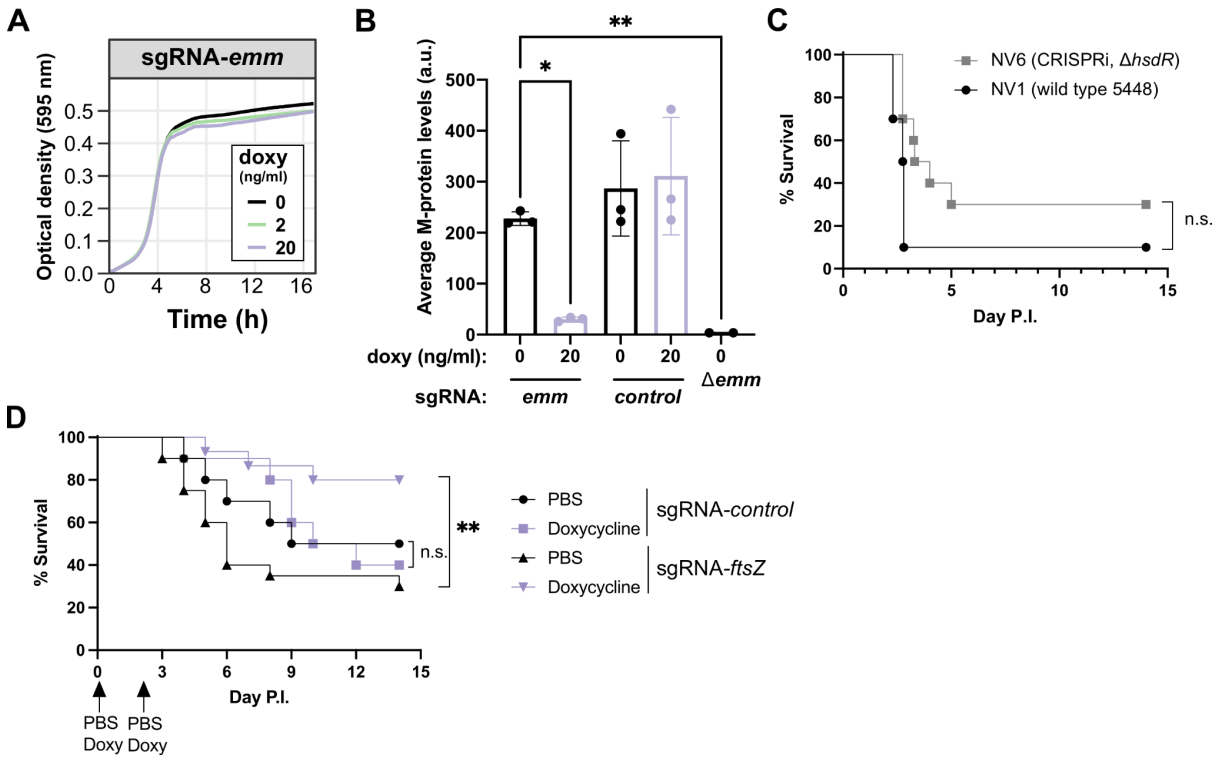

Fig. 5: Efficient depletion of M-protein and *in vivo* CRISPRi in GAS. (**A**) Strain NV25 (NV6+pDC-sgRNA-*emm*) was grown in THB containing 2 µg/ml of chloramphenicol at 37°C in microtiter plates in the presence of various concentrations of doxycycline. (**B**) Strains NV25 (sgRNA-emm), NV26 (sgRNA-control), and M protein knockout GAS M1T1 5448 were grown in THB to mid-logarithmic growth in the presence or absence of 20 ng/ml doxycycline. Bacteria were immunostained using M protein antisera and analyzed by flow cytometry as described in the Methods. (**C**) Strains NV1 (wild type GAS 5448) and NV6 (*cas9::tetM*, *tetR*, Ptet-*dcas9*, *hsdR::ery*) were grown in THB at 37°C and 1-3*10^8 CFU were used to infect CD-1 mice IP (10 mice per group). Disease score and survival was followed for 14 days. There was no statistical significant (n.s.) difference in virulence between both strains (Mantel-Cox Log Rank test). (**D**) Strains NV26 (NV6+pDC-sgRNA-*control*) and NV19 (NV6+pDC-sgRNA-*ftsZ*) were grown in THB containing 2 µg/ml of chloramphenicol at 37°C and 1-3*10^8 CFU were used to infect CD-1 mice IP (10 mice per group). Disease score and survival was followed for 14 days. Doxy-induced mice infected with NV19 showed a statistically significant increased survival (** p = 0.0027, Mantel-Cox Log Rank test).

330 **Discussion**

331 GAS remains a predominant cause of bacterial infections worldwide. While significant strides have
332 been made in understanding GAS physiology and its interactions with the host (1, 17), fundamental
333 insights into its basic cell biology lag behind. Such knowledge is crucial for the development of vaccines
334 and the identification of novel drug targets. The existing knowledge gap is largely attributed to the
335 challenges in genetic manipulation of pathogenic GAS strains and the absence of a modern molecular
336 toolbox. Here, we bridge this gap by creating a highly transformable, fully virulent M1T1 GAS strain,
337 establishing a titratable doxy/tetracycline/aTc-inducible system, and introducing CRISPRi for
338 controlled gene expression in GAS.

339 By employing a non-polar *hsdR* mutant, sgRNAs can be directly cloned into GAS without the
340 need for an *E. coli* intermediate. This streamlined approach makes it possible to obtain a specific gene
341 depletion within days, as opposed to weeks or months (10). Utilizing readily available oligonucleotides,
342 following the design outlined in Table S1, and using previously prepared electrocompetent NV6 cells
343 (*hsdR::ery*, *cas9::tetM*, *tetR*, Ptet-*dcas9*) a CRISPRi experiment can be conducted in as little as three
344 days. Importantly, we show that not only is this CRISPRi system functional *in vitro*, but it can be
345 efficiently induced in a murine infection model, simply by administering doxy to the animal.

346 The tools and methodologies outlined in this study can markedly enhance the throughput by
347 which GAS research may be performed, and we foresee that genome-wide CRISPRi screens (CRISPRi-
348 seq) will soon become feasible for GAS (41). CRISPRi and CRISPRi-seq offer advantages over existing
349 TrAsh, Tn-seq and TRADIS workflows for GAS (11, 18, 47) since they enable the examination of
350 essential gene functions and the performance of titratable drug-gene interaction studies. Moreover, we
351 anticipate that the P*tet-dcas9* cassette and pDC-sgRNA plasmid system can be readily applied to other
352 low GC-rich Gram-positive bacteria.

353 Annotation databases like SubtiWiki (48), EcoCyc (49), and PneumoBrowse (50) have
354 significantly accelerated gene discovery, functional analysis, and hypothesis-driven studies for these
355 bacteria. In this work, we introduce SpyBrowse (https://veeninglab.com/SpyBrowse), a public domain
356 resource enabling users to explore the newly assembled GAS *S. pyogenes* 5448 NV1 genome.

357 SpyBrowse facilitates the inspection of encoded features, regulatory elements, repeat regions, and other
358 valuable properties. It also provides information on sgRNA binding sites and links to useful
359 bioinformatic resources such as Alphafold predictions (51) (via Uniprot (14)) and PaperBlast (15).
360 SpyBrowse will undergo regular updates and is fully capable of incorporating various omics data and
361 improved genome annotations, akin to the approach taken by PneumoBrowse (50). The methodologies
362 presented in this study can serve as a roadmap for developing CRISPRi in other challenging-to-
363 transform bacteria. Together with SpyBrowse, they should represent a valuable resource for researchers
364 in the GAS field.
365

366 ## Methods

367 **Bacterial strains and culture conditions.**

368 All strains, plasmids and primers used are listed in Supplementary Table S2 and Supplementary Table
369 S3. All GAS strains in this study are derivatives of *S. pyogenes* 5448 (12) and are listed in
370 Supplementary Table S2. Strains were grown in liquid THB (Hardy Diagnostics (or Oxoid THB for
371 Fig. 1C, right panel) without aeration at 37˚C. The IPTG-inducible promoter on pAV488 was activated
372 with 1 mM IPTG (β-D-1-thiogalactopyranoside, Sigma-Aldrich). Electrocompetent GAS cells were
373 made by overnight growth in THB + 0.6% glycine followed by 1:10 dilution in fresh THB + 0.6%
374 glycine. If required, 1 mM of IPTG was used to induce recombineering from pAV488 (Varble,
375 laboratory collection) when cells reached an OD600 of 0.15. At OD600 of 0.3, cells were centrifuged
376 (4000 rpm, 10 min, 4°C) and washed four times with 0.625 M Sucrose before resuspending in 20%
377 glycerol and stored at -80˚C in 50 µl aliquots. For electroporation, DNA was added to one 50 µl aliquot
378 of electrocompetent cells on ice for 5 min before transferring to a 1 mm electroporation cuvette
379 (Genesee Scientific). After electroporation (Eppendorf 2510, 1.7 kilovolts), cells were incubated in
380 THB + 0.25 M Sucrose for 2 h before overnight antibiotic selection on THA (37˚C). When appropriate,
381 the medium was supplemented with the following antibiotics: chloramphenicol (2 $\mu g.mL^{-1}$),
382 erythromycin (0.5 $\mu g.mL^{-1}$), kanamycin (400 $\mu g.mL^{-1}$), and tetracycline (0.5 $\mu g.mL^{-1}$). Genomic GAS

383 DNA was prepared using the Zymo Quick-DNA Fungal/Bacterial Miniprep Kit (4 ml of overnight
384 culture was used as input).
385 Plasmid pDC-sgRNA was made in *E. coli* strain MC1061 (MClab) grown in LB medium at
386 37°C with aeration; 5 µg.mL^{-1} chloramphenicol was added when appropriate.
387
388 **Recombineering, plasmid and strain construction**
389 Recombineering plasmid pAV488 (Varble, laboratory collection) was transformed by electroporation
390 to wildtype 5448 (strain NV1) selecting on chloramphenicol resulting in strain NV2 (Supplementary
391 Table S2). Next, the recombineering enzymes Gam, ERF recombinase and single stranded DNA
392 binding protein encoded on pAV488 were induced with 1 mM of IPTG and cells were made
393 electrocompetent and stored at -80˚C. To generate an *hsdR* replacement mutant, an erythromycin
394 cassette without promoter and terminator but with its own RBS was amplified by PCR using primers
395 ONV31/ONV32 (Supplementary Table S3) using chromosomal DNA of strain VL4321 (52) as
396 template. The *hsdR* upstream and downstream regions were amplified using chromosomal DNA of
397 strain NV1 as template using primers ONV29/ONV30 and ONV33/ONV34, respectively (**Fig. 1**). The
398 three PCR fragments were purified (Zymo DNA Clean and Concentrator kit: 'Zymo kit') and used in a
399 1:1:1 molar ratio Golden Gate assembly reaction with BsaI (NEB) and T4 ligase (NEB) for 50 cycles
400 of 1.5 min at 37°C followed by 3 min at 16°C. Enzymes were inactivated at 80°C for 10 min. The
401 assembly was purified (Zymo kit) and 1 µl was used as a template in a PCR using primers
402 ONV29/ONV34. The resulting 3431 bps fragment was purified (Zymo kit) and 10 µl was used to
403 transform electrocompetent NV2 cells. Erythromycin resistant colonies were selected and used for
404 further analysis resulting in strain NV3 (*hsdR::ery*, pAV488). Strain NV3 was cured from plasmid
405 pAV488 by growing it overnight in THB with 1 mM IPTG (without chloramphenicol) and restreaking
406 single colonies, resulting in strain NV28 (*hsdR::ery*).
407 Strain NV4 (*hsdR::ery*, *cas9::kan*, pAV488) was made by amplifying approximately 1kb
408 upstream and downstream of the *cas9* locus (**Fig. 2B)** using primers ONV1/ONV2 and ONV5/OV6,
409 respectively, using chromosomal DNA of strain NV1 as template. A kanamycin resistance cassette
410 including promoter and terminator was amplified from plasmid pAV258 (Varble laboratory collection)

411 using primers ONV3/ONV4. The three PCR fragments were purified (Zymo kit) and used in a 1:1:1
412 molar ratio Golden Gate assembly reaction with AarI (ThermoFisher) and T4 ligase (NEB) for 50 cycles
413 of 1.5 min at 37°C followed by 3 min at 16°C. Enzymes were inactivated at 80°C for 10 min. The
414 assembly was purified (Zymo kit) and 1 µl was used as a template in a PCR using primers
415 ONV1/ONV6. The resulting 3995 bps fragment was purified (Zymo kit) and 10 µl was used to
416 transform electrocompetent NV3 cells. Kanamycin resistant colonies were selected and used for further
417 analysis resulting in strain NV4.

418 Strain NV6 (*hsdR::ery*, *cas9::tetM, tetR,* Ptet-*dcas9*) was constructed by amplifying
419 approximately 1 kb upstream and downstream of the *cas9* locus using primers ONV1/ONV9 and
420 ONV6/ONV12, respectively, using chromosomal DNA of strain NV1 as template. The *tetM-tetR-Ptet-*
421 *dcas9* cassette was amplified from chromosomal DNA of strain VL3469 (37) using primers
422 ONV10/ONV11. The three PCR fragments were purified (Zymo kit) and used in a 1:1:1 molar ratio
423 Golden Gate assembly reaction with AarI (ThermoFisher) and T4 ligase (NEB) for 60 cycles of 1.5 min
424 at 37°C followed by 3 min at 16°C. Enzymes were inactivated at 80°C for 10 min. The 9774 bps ligation
425 product was cut from gel and purified (Zymoclean Gel DNA recovery kit) and directly used to transform
426 electrocompetent NV4 cells. Tetracycline resistant colonies were selected and plasmid cured, resulting
427 in strain NV6. Since NV6 cells harbor the *tetM* resistance marker, growth is not perturbed by doxy upon
428 inducing with 20 ng/ml.

429 Plasmid pDC-sgRNA was constructed as follows: A PCR using primers ONV21/ONV22 and
430 plasmid pDC123 (24) as template was performed to obtain the vector backbone. The *sgRNA-mCherry*
431 cassette flanked by the Illumina read 1 and read 2 sequences were amplified using plasmid pVL4930
432 (Veening laboratory collection) as template with primers ONV23/ONV24. Next, the two fragments
433 were purified (Zymo kit) and used in a 1:1 molar ratio Golden Gate assembly reaction with BsaI-HF2
434 (NEB) and T4 ligase (NEB) for 50 cycles of 1.5 min at 37°C followed by 3 min at 16°C. Enzymes were
435 inactivated at 80°C for 10 min. The ligation product was used to transform chemically competent *E.*
436 *coli* MC1061 (MCLab). A pink, mCherry-expressing chloramphenicol resistant colony was restreaked
437 and selected for further analysis resulting in *E. coli* strain pDC-sgRNA (Supplementary Table S2).
438 Plasmid pDC-sgRNA was purified (Qiagen miniprep kit) and verified by nanopore sequencing

439 (Plasmidsaurus). Note that *mCherry*, and the subsequent sgRNA, is driven by the strong constitutive P3
440 promoter (43) and that all cloned sgRNAs will have adenine as initiating nucleotide (+1) (**Fig. 2A**),
441 ensuring strong expression regardless of spacer sequence (41, 50).

442 To construct GAS strains NV19, NV22, NV25 and NV26, complementary oligos
443 ONV60/ONV61, ONV66/ONV67, ONV72/ONV73 and ONV74/ONV75, respectively, were annealed
444 and phosphorylated. Briefly, 2.5 µl of each complementary oligo (at 100 µM concentration) were
445 annealed in a 50 µl reaction containing 5 µl 10x TEN buffer (100 mM Tris-HCl pH8, 10 mM EDTA,
446 500 mM NaCl) for 5 min at 95°C and slowly cooled to room temperature. Next, 1 µl of the annealed
447 oligos were phosphorylated in a 10 µl reaction containing 0.25 µl T4 PNK (10000 units/ml, NEB) and
448 1 µl 10x T4 ligase buffer for 40 min at 37°C before heat-inactivation at 65°C for 20 min. Finally, the
449 phosphorylated annealed oligos were diluted 10-fold (to 0.05 µM DNA) ready to use for ligation. To
450 generate the digested pDC-sgRNA vector, 1 µl of plasmid pDC-sgRNA was used as a template in a
451 PCR using outward facing primers ONV76/ONV77 binding within the *mCherry* sequence. The PCR
452 product was incubated with EcoRV (NEB) that cuts inside *mCherry* for 30 min at 37°C to linearize any
453 remaining template DNA. Next, the reaction was purified (Zymo kit) and digested with BsmBI-HF
454 (NEB) at 55°C for 3h followed by purification using the Zymo kit. 100 ng of pure digested pDC-sgRNA
455 was used in a 15 µl ligation reaction containing 3.5 µl of the 0.05 µM annealed phosphorylated primers.
456 Ligation was performed for 1h at RT or overnight at 16°C. Finally, 7 µl of the ligation mixture was
457 used to transform electrocompetent cells of strain NV6 by electroporation, resulting in strains NV19,
458 NV22, NV25 and NV26, respectively. Plasmids were isolated by miniprep (Qiagen) and correct spacer
459 sequences were verified by Sanger sequencing using primer ONV92.

460

461 **Microtiter plate-based growth assay**

462 Overnight GAS cultures grown in THB medium at 37°C were diluted 1:20 in the morning in fresh THB
463 until mid-exponential growth (OD_{600nm} = 0.3) with no inducer at 37°C, after which they were diluted to
464 OD_{600nm} = 0.004 in 250ul of fresh THB medium supplemented with doxy when appropriate inside 96-
465 well flat bottom microtiter plates (Costar 3370) covered with Breath-Easy film (Sigma) to prevent
466 evaporation. Cellular growth was then monitored every 10 min at either 37°C in a microtiter plate reader

467 (TECAN Infinite F200 Pro). Each growth assay was performed in triplicate and the average of the
468 triplicate values with standard errors of the mean were plotted using BactExtract (53).
469
470 **DIC and fluorescence microscopy**
471 GAS cells were grown in THB medium at 37°C to an OD_{600nm} = 0.3 without any inducer and diluted 50
472 times in fresh THB medium supplemented, when appropriate, with 20 $ng.mL^{-1}$ doxy (for activation of
473 dCas9). After 3 h, 1 mL of culture was collected. For membrane staining, 5 $\mu g.mL^{-1}$ of Nile red
474 (Invitrogen) was added and for DAPI staining, 1 $\mu g.mL^{-1}$ DAPI (Sigma-Aldrich) was added to the cells
475 and incubated for 5 min at room temperature prior to centrifugation. Cells were washed twice with 1
476 mL PBS and re-suspended into 50 µL PBS. 1 µL of cells were then spotted onto PBS agarose (1%)
477 pads in 10-well multitest microscope slides (MP Biomedicals). Microscopy acquisition was performed
478 using a Zeiss M1 upright microscope with a 100x oil-immersion objective. Images were processed using
479 Fuji (54).
480
481 **Genome sequencing, annotation, methylation analysis and spacer design**
482 Strain NV1 (GAS 5448, Nizet lab collection) was sequenced, assembled, and annotated by
483 Plasmidsaurus, Inc. according to the protocols listed on the Plasmidsaurus website
484 (https://www.plasmidsaurus.com/faq/#bact-assembly). In addition, strains NV1, NV28 and NV6 were
485 also sequenced using the PacBio Sequel II instrument at the Lausanne Genomics Facility. Read
486 demultiplexing and quality control were performed with SMRTLink version 11.0
487 (https://www.pacb.com/support/software-downloads/). The microbial genome assembly pipeline in this
488 toolkit was used to assemble genomes and identify methylation motifs. Assemblies were circularized
489 with circlator (55). Structural variants were detected with pbmm2 version 1.13.1 (56) and pbsv version
490 2.9.0 using default settings then confirmed manually. Whole genome alignments were performed and
491 visualized in Mauve (57). This revealed a large genome inversion of 1,475,033 base pairs. Prokka (27)
492 was used to annotate the NV1 PacBio genome and used to design a unique sgRNA (see Supplementary
493 Table S1) for every genetic feature as described (41). Genome sequences confirmed correct gene
494 replacement of *hsdR* in NV6 and NV28 and correct integration of Ptet-*dcas9* at the *cas9* locus in NV6.

495 Besides the large genome inversion and several smaller insertions, the genome differs on the following
496 sites from the publicly available 5448 genome sequence (25) (GenBank: CP008776.1): NV1
497 numbering: 196'187 t-->c, 196'188 c-->t, 196'385 g-->t, 196'446 t-->c, 196'452 t-->c, 296'177 a-->c,
498 296'508 g-->t, 296'568 t-->c, 296'575 t-->c, 334'494 c-->a, 334'434 a-->g, 334'427 a-->g, 1'308'897
499 g-->a, 1'310'949 a-->c, 1'518'946 g-->a, 1'518'953 g-->a, 1'519'013 a-->c, 1'565'892 a-->t,
500 1'599'979 a-->c, 1'672'223 a-->g, 1'672'224 g-->a). These SNPs are mainly related to the ISAs1-like
501 elements. The polished NV1 genome was further annotated by the NCBI Prokaryotic Genome
502 Annotation Pipeline (PGAP) and is available with accession number CP140117.2 and visualized
503 through SpyBrowse (see below).
504
505 **SpyBrowse**
506 SpyBrowse (https://veeninglab.com/SpyBrowse) is based on JBrowse (13). Features were divided over
507 3 annotation tracks: (i) genome, (ii) genes, and (iii) designed sgRNAs.
508
509 **Quantifications and statistical analysis**
510 Data analysis was performed using R (R version 4.2.2) and Prism (Version 10.0.3, Graphpad). Data
511 shown are represented as the mean of at least three replicates ± SEM if data came from one experiment
512 with replicated measurement, and ± SD if data came from separate experiments.
513
514 **Flow cytometry**
515 NV25 (sgRNA-*emm*), NV26 (sgRNA-control), and M protein knockout GAS M1T1 5448 were grown
516 overnight in THB with chloramphenicol for NV25 and NV26. Cultures were diluted 1:10 from
517 overnights in THB (without chloramphenicol) and grown to mid-logarithmic phase (OD_{600} = 0.4) for
518 2.5 hours. During this time, NV25 and NV26 were grown +/- 20 ng/ml doxycycline to induce the
519 CRISPRi system. Bacteria were washed in PBS and incubated in 10% donkey serum at room
520 temperature. Rabbit M protein antisera (Vaxcyte) was added at 2% final concentration for 1 hour at
521 room temperature. Bacteria were washed with PBS and then incubated in 1:200 donkey anti-rabbit IgG
522 conjugated AlexaFluor 488 fluorophore (Thermo Fisher #21206) for 30 minutes at room temperature.

523 Samples were washed in PBS and run on a BD FACSCalibur. Flow cytometry data were analyzed with
524 FlowJo v. 10.8.2 (Tree Star, Inc.).
525
526 **Mouse infection experiments**
527 Eight-week old female CD1 mice (Charles River Laboratories) were infected intraperitoneally with 1-
528 3 x 10^8 CFU in 100 µl of each GAS engineered strain (n = 20 per strain). One hour prior to infection,
529 mice were injected intraperitoneally with either 25 µg doxycycline (n = 10) or PBS (n = 10). 48h
530 following infection a second 25 µg doxy dose was administered i.p. Mortality was observed daily for
531 14 days post infection. Mice were housed on a 12 hour light/dark schedule, fed a 2020x diet (Envigo),
532 and received acidified water. Prior to experimentation, mice were randomized into cages with no more
533 than 5 mice per cage. Mouse experiments were approved by the UC San Diego Institutional Animal
534 Care and Use Committee (Protocol #S00227M) in compliance with federal regulations and were
535 conducted with oversight from veterinary professionals.
536
537 **Data availability**
538 The data that support the findings of this study are incorporated in the manuscript and its supporting
539 information. Pacbio genome sequences, assemblies, and sequencing reads are available at NCBI under
540 BioProject accession number PRJNA1050251.
541
542 **Acknowledgements**
543 We thank the members of the Nizet and Veening groups for valuable discussions. We thank Doran
544 Pauka for help with SpyBrowse. We thank the Lausanne Genomic Technologies Facility for SMRT
545 sequencing and continued support. J.W.V. was supported for this project by the Fondation Herbette and
546 by the Swiss National Science Foundation (SNSF) (Scientific Exchange grant IZSEZ0_213879). Work
547 in the lab of J.W.V. was supported by SNSF grants 310030_192517, 310030_200792 and
548 51NF40_180541.
549

550 **Author contributions**

551 J.W.V. wrote the paper with input from all authors. J.W.V., E.B., A.S., P.S.G., S.D., J.L.B. and A.M.B.

552 performed the experiments. J.W.V. and V.N. designed, analyzed and interpreted the data.

553

554 **Competing interests**

555 The authors declare no competing interests.

556

557 **Supplementary information**

558 Supplementary Table S1: GAS 5448 (NV1) genome-wide sgRNA design

559 Supplementary Table S2: Strains and plasmids

560 Supplementary Table S3: Oligonucleotides

561

562 **References**

563 1. J. N. Cole, T. C. Barnett, V. Nizet, M. J. Walker, Molecular insight into invasive group A
564 streptococcal disease. *Nat. Rev. Microbiol.* **9**, 724–736 (2011).

565 2. T. J. Mitchell, The pathogenesis of streptococcal infections: from tooth decay to meningitis. *Nat.*
566 *Rev. Microbiol.* **1**, 219–230 (2003).

567 3. J. R. Carapetis, A. C. Steer, E. K. Mulholland, M. Weber, The global burden of group A
568 streptococcal diseases. *Lancet Infect. Dis.* **5**, 685–694 (2005).

569 4. A. P. Ralph, J. R. Carapetis, Group a streptococcal diseases and their global burden. *Curr. Top.*
570 *Microbiol. Immunol.* **368**, 1–27 (2013).

571 5. A. Sims Sanyahumbi, S. Colquhoun, R. Wyber, J. R. Carapetis, "Global Disease Burden of
572 Group A Streptococcus" in *: Basic Biology to Clinical Manifestations*, J. J. Ferretti, D. L.
573 Stevens, V. A. Fischetti, Eds. (University of Oklahoma Health Sciences Center, 2016).

574 6. A. F. Johnson, C. N. LaRock, Antibiotic Treatment, Mechanisms for Failure, and Adjunctive
575 Therapies for Infections by Group A. *Front. Microbiol.* **12**, 760255 (2021).

576 7. J. B. Dale, M. J. Walker, Update on group A streptococcal vaccine development. *Curr. Opin.*
577 *Infect. Dis.* **33**, 244–250 (2020).

578 8. D. J. McMillan, *et al.*, Updated model of group A Streptococcus M proteins based on a
579 comprehensive worldwide study. *Clin. Microbiol. Infect.* **19**, E222–9 (2013).

580 9. R. K. Aziz, M. Kotb, Rise and persistence of global M1T1 clone of Streptococcus pyogenes.
581 *Emerg. Infect. Dis.* **14**, 1511–1517 (2008).

582 10. Y. Le Breton, K. S. McIver, Genetic Manipulation of Streptococcus pyogenes (The Group A
583 Streptococcus, GAS). *Curr. Protoc. Microbiol.* **30**, 9D.3.1–9D.3.29 (2013).

584 11. Y. Le Breton, *et al.*, Essential Genes in the Core Genome of the Human Pathogen Streptococcus
585 pyogenes. *Sci. Rep.* **5**, 9838 (2015).

586 12. S. Chatellier, *et al.*, Genetic relatedness and superantigen expression in group A streptococcus
587 serotype M1 isolates from patients with severe and nonsevere invasive diseases. *Infect. Immun.*
588 **68**, 3523–3534 (2000).

589 13. R. Buels, *et al.*, JBrowse: a dynamic web platform for genome visualization and analysis.
590 *Genome Biol.* **17**, 66 (2016).

591 14. The UniProt Consortium, *et al.*, UniProt: the Universal Protein Knowledgebase in 2023. *Nucleic*
592 *Acids Res.* **51**, D523–D531 (2022).

593 15. M. N. Price, A. P. Arkin, PaperBLAST: Text Mining Papers for Information about Homologs.
594 *mSystems* **2** (2017).

595 16. Y. Le Breton, *et al.*, Genome-wide discovery of novel M1T1 group A streptococcal determinants
596 important for fitness and virulence during soft-tissue infection. *PLoS Pathog.* **13**, e1006584
597 (2017).

598 17. S. Brouwer, *et al.*, Pathogenesis, epidemiology and control of Group A Streptococcus infection.
599 *Nat. Rev. Microbiol.* **21**, 431–447 (2023).

600 18. Y. Le Breton, *et al.*, Genome-wide identification of genes required for fitness of group A
601 Streptococcus in human blood. *Infect. Immun.* **81**, 862–875 (2013).

602 19. M. B. Finn, K. M. Ramsey, H. J. Tolliver, S. L. Dove, M. R. Wessels, Improved transformation
603 efficiency of group A Streptococcus by inactivation of a type I restriction modification system.
604 *PLoS One* **16**, e0248201 (2021).

605 20. T. M. Nye, *et al.*, DNA methylation from a Type I restriction modification system influences
606 gene expression and virulence in Streptococcus pyogenes. *PLoS Pathog.* **15**, e1007841 (2019).

607 21. S. DebRoy, *et al.*, Characterization of the Type I Restriction Modification System Broadly
608 Conserved among Group A Streptococci. *mSphere* **6**, e0079921 (2021).

609 22. R. Okada, *et al.*, Emergence of type I restriction modification system-negative emm1 type
610 Streptococcus pyogenes clinical isolates in Japan. *APMIS* **122**, 914–921 (2014).

611 23. R. A. Sorg, C. Gallay, L. Van Maele, J.-C. Sirard, J.-W. Veening, Synthetic gene-regulatory
612 networks in the opportunistic human pathogen. *Proc. Natl. Acad. Sci. U. S. A.* **117**, 27608–27619
613 (2020).

614 24. D. O. Chaffin, C. E. Rubens, Blue/white screening of recombinant plasmids in Gram-positive
615 bacteria by interruption of alkaline phosphatase gene (phoZ) expression. *Gene* **219**, 91–99
616 (1998).

617 25. A. Fiebig, *et al.*, Comparative genomics of Streptococcus pyogenes M1 isolates differing in
618 virulence and propensity to cause systemic infection in mice. *Int. J. Med. Microbiol.* **305**, 532–
619 543 (2015).

620 26. S. Khazaal, R. Al Safadi, D. Osman, A. Hiron, P. Gilot, Data on the link between genomic
621 integration of IS and lineage of the strain obtained by bioinformatic analyses of sequenced
622 genomes of available at the National Center for Biotechnology Information database. *Data Brief*

28, 105066 (2020).

27. T. Seemann, Prokka: rapid prokaryotic genome annotation. *Bioinformatics* **30**, 2068–2069 (2014).

28. A. Vigouroux, D. Bikard, CRISPR Tools To Control Gene Expression in Bacteria. *Microbiol. Mol. Biol. Rev.* **84** (2020).

29. H. Todor, M. R. Silvis, H. Osadnik, C. A. Gross, Bacterial CRISPR screens for gene function. *Curr. Opin. Microbiol.* **59**, 102–109 (2021).

30. R. Zhang, W. Xu, S. Shao, Q. Wang, Gene Silencing Through CRISPR Interference in Bacteria: Current Advances and Future Prospects. *Front. Microbiol.* **12**, 635227 (2021).

31. S. N. Call, L. B. Andrews, CRISPR-Based Approaches for Gene Regulation in Non-Model Bacteria. *Front Genome Ed* **4**, 892304 (2022).

32. D. Bikard, *et al.*, Programmable repression and activation of bacterial gene expression using an engineered CRISPR-Cas system. *Nucleic Acids Res.* **41**, 7429–7437 (2013).

33. L. S. Qi, *et al.*, Repurposing CRISPR as an RNA-guided platform for sequence-specific control of gene expression. *Cell* **152**, 1173–1183 (2013).

34. A. Le Rhun, A. Escalera-Maurer, M. Bratovič, E. Charpentier, CRISPR-Cas in Streptococcus pyogenes. *RNA Biol.* **16**, 380–389 (2019).

35. M. Geissendörfer, W. Hillen, Regulated expression of heterologous genes in Bacillus subtilis using the Tn10 encoded tet regulatory elements. *Appl. Microbiol. Biotechnol.* **33**, 657–663 (1990).

36. J. V. Bugrysheva, B. J. Froehlich, J. A. Freiberg, J. R. Scott, The histone-like protein Hlp is essential for growth of Streptococcus pyogenes: comparison of genetic approaches to study essential genes. *Appl. Environ. Microbiol.* **77**, 4422–4428 (2011).

37. X. Liu, *et al.*, Exploration of Bacterial Bottlenecks and Streptococcus pneumoniae Pathogenesis by CRISPRi-Seq. *Cell Host Microbe* **29**, 107–120.e6 (2021).

38. I. M. Redelsperger, *et al.*, Stability of Doxycycline in Feed and Water and Minimal Effective Doses in Tetracycline-Inducible Systems. *J. Am. Assoc. Lab. Anim. Sci.* **55**, 467–474 (2016).

39. X. Liu, *et al.*, A conserved antigen induces respiratory Th17-mediated serotype-independent protection against pneumococcal superinfection. *bioRxiv*, 2023.07.07.548156 (2023).

40. S. A. Lacks, P. Lopez, B. Greenberg, M. Espinosa, Identification and analysis of genes for tetracycline resistance and replication functions in the broad-host-range plasmid pLS1. *J. Mol. Biol.* **192**, 753–765 (1986).

41. V. de Bakker, X. Liu, A. M. Bravo, J.-W. Veening, CRISPRi-seq for genome-wide fitness quantification in bacteria. *Nat. Protoc.* **17**, 252–281 (2022).

42. J. van Gestel, J. S. Hawkins, H. Todor, C. A. Gross, Computational pipeline for designing guide RNAs for mismatch-CRISPRi. *STAR Protoc* **2**, 100521 (2021).

43. R. A. Sorg, O. P. Kuipers, J.-W. Veening, Gene expression platform for synthetic biology in the human pathogen Streptococcus pneumoniae. *ACS Synth. Biol.* **4**, 228–239 (2015).

44. M. L. White, P. J. Eswara, Has More than a (Z Anchor) Ring to It! *J. Bacteriol.* **203** (2021).

662 45. S. Kifayat, *et al.*, Filamentous temperature sensitive mutant Z: a putative target to combat
663 antibacterial resistance. *RSC Adv.* **13**, 11368–11384 (2023).

664 46. D. J. Haydon, *et al.*, An inhibitor of FtsZ with potent and selective anti-staphylococcal activity.
665 *Science* **321**, 1673–1675 (2008).

666 47. L. Zhu, *et al.*, Novel Genes Required for the Fitness of in Human Saliva. *mSphere* **2** (2017).

667 48. R. H. Michna, B. Zhu, U. Mäder, J. Stülke, SubtiWiki 2.0--an integrated database for the model
668 organism Bacillus subtilis. *Nucleic Acids Res.* **44**, D654–62 (2016).

669 49. I. M. Keseler, *et al.*, The EcoCyc database: reflecting new knowledge about Escherichia coli K-
670 12. *Nucleic Acids Res.* **45**, D543–D550 (2017).

671 50. J. Slager, R. Aprianto, J.-W. Veening, Deep genome annotation of the opportunistic human
672 pathogen Streptococcus pneumoniae D39. *Nucleic Acids Res.* **46**, 9971–9989 (2018).

673 51. J. Jumper, *et al.*, Highly accurate protein structure prediction with AlphaFold. *Nature* **596**, 583–
674 589 (2021).

675 52. A.-S. Rueff, *et al.*, Synthetic genetic oscillators demonstrate the functional importance of
676 phenotypic variation in pneumococcal-host interactions. *Nat. Commun.* **14**, 7454 (2023).

677 53. J. Dénéréaz, J.-W. Veening, BactEXTRACT: an R Shiny app to quickly extract, plot and analyse
678 bacterial growth and gene expression data. *Access Microbiol* **6** (2024).

679 54. J. Schindelin, *et al.*, Fiji: an open-source platform for biological-image analysis. *Nat. Methods* **9**,
680 676–682 (2012).

681 55. M. Hunt, *et al.*, Circlator: automated circularization of genome assemblies using long sequencing
682 reads. *Genome Biol.* **16**, 294 (2015).

683 56. GitHub - PacificBiosciences/pbmm2: A minimap2 frontend for PacBio native data formats.
684 *GitHub* (December 16, 2023).

685 57. A. E. Darling, A. Tritt, J. A. Eisen, M. T. Facciotti, Mauve assembly metrics. *Bioinformatics* **27**,
686 2756–2757 (2011).

687